

## Research Article

# Mechanical Properties of SiO<sub>2</sub>-Coated Carbon Fiber-Reinforced Mortar Composites with Different Fiber Lengths and Fiber Volume Fractions

Gwang-Hee Heo,<sup>1</sup> Jong-Gun Park<sup>2</sup>,<sup>3</sup> Ki-Chang Song,<sup>3</sup> Jong-Ho Park,<sup>3</sup>  
and Hyung-Min Jun<sup>4</sup>

<sup>1</sup>Department of International Civil and Plant Engineering, Konyang University, 121 Daehak-Ro, Nonsan-Si, Chungnam-Do 32992, Republic of Korea

<sup>2</sup>Public Safety Research Center (PSRC), Konyang University, 121 Dachak-Ro, Nonsan-Si, Chungnam-Do 32992, Republic of Korea

<sup>3</sup>Department of Biomedical Materials, Konyang University, 158 Gwanjedong-Ro, Seo-Gu, Daejeon Metropolitan-Si 35365, Republic of Korea

<sup>4</sup>Department of Disaster and Safety Engineering, Konyang University, 121 Dachak-Ro, Nonsan-Si, Chungnam-Do 32992, Republic of Korea

Correspondence should be addressed to Jong-Gun Park; 2630@hanmail.net

Received 28 May 2020; Revised 9 July 2020; Accepted 22 September 2020; Published 12 October 2020

Academic Editor: Peng Zhang

Copyright © 2020 Gwang-Hee Heo et al. This is an open access article distributed under the Creative Commons Attribution License, which permits unrestricted use, distribution, and reproduction in any medium, provided the original work is properly cited.

In the present study, SiO<sub>2</sub> particles were coated on the surface of carbon fibers by means of chemical reaction of silane coupling agent (glycidoxypropyl trimethoxysilane, GPTMS) and colloidal SiO<sub>2</sub> sol to improve the interfacial bonding force between fibers and matrix in cement matrix. The surface of the modified carbon fibers was confirmed through a scanning electron microscope (SEM). The mechanical properties of SiO<sub>2</sub>-coated carbon fiber mortar and uncoated carbon fiber mortar with different fiber lengths (6 mm and 12 mm) and fiber volume fractions (0.5%, 1.0%, 1.5%, and 2.0%) were compared and analyzed. The experimental results show that the flow values of the carbon fiber mortar were greatly disadvantageous in terms of fluidity due to the nonhydrophilicity of fibers and fiber balls, and the unit weight decreased significantly as the fiber volume fractions increased. However, the air content increased more or less. In addition, regardless of whether the fibers were coated, the compressive strength of carbon fiber-reinforced mortar (CFRM) composite specimens tended to gradually decrease as the fiber volume fractions increased. On the other hand, in case of the SiO<sub>2</sub>-coated CFRM composite specimens, the flexural strength was significantly increased compared to uncoated CFRM composite specimens and plain mortar specimens, and the highest flexural strength was obtained at 12 mm and 1.5%, particularly. It can be seen that the new carbon fiber surface modification method employed in this study was very effective in enhancing the flexural strength as cement-reinforcing materials.

## 1. Introduction

Fiber-reinforced cement composites (FRCCs) are manufactured by incorporating short fibers, which can suppress the opening and propagation of cracks due to the bridging action of fibers. It not only increases ductility in tension and compression but also provides improved safety performance for dynamic load, impact-explosion, etc. [1–6]. Currently,

the main reinforcing materials of fiber-reinforced cement-based composite materials are steel fiber, polypropylene fiber, polyvinyl alcohol (PVA) fiber, carbon fiber, glass fiber, basalt fiber, and cellulose fiber [7–10].

Figure 1 shows the roles of fibers embedded in cement matrix: (a) cracking occurs in cement matrix, (b) cracking is suppressed due to the increased bond between fibers and matrix, (c) the phenomenon of “strain-softening” or “strain-

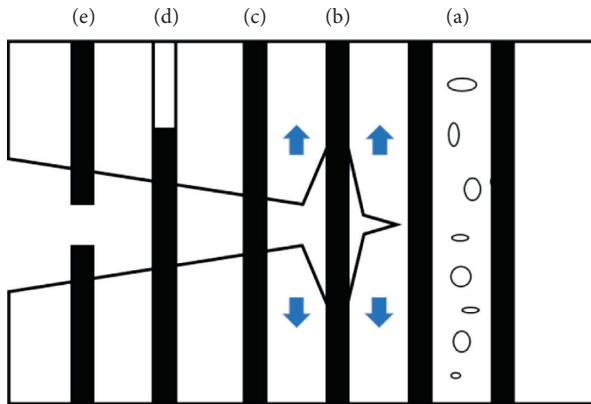


FIGURE 1: The roles of fiber embedded in cement matrix: (a) matrix cracking, (b) fiber/matrix debonding, (c) fiber bridging, (d) fiber pull-out, and (e) fiber failure.

hardening” by suppressing crack propagation owing to bridging action between fibers and matrix is shown after cracking in cement matrix, (d) fibers are pulled-out from cement matrix, and (e) the performance of FRCC is degraded by fiber failure. As seen above, it has been reported that the mechanical performance of cement-based composites can be improved by effectively preventing the propagation of cracks by stress through bonding between fibers and matrix as well as by controlling crack propagation by means of fiber bridging, fiber debonding, fiber pull-out, fiber failure, etc. [11–16]. Moreover, it is noted that the bond performance between fibers and matrix is very closely related to the performance of FRCC and that the material and surface shape of fibers, matrix strength, etc. play a vastly important role in the interfacial bonding force between fibers and matrix [17, 18]. Such interfacial properties of fibers are directly connected with effective improvement of the flexural performance (flexural strength or toughness) of the cement-based composites and exercise a substantial influence on the flexural and tensile fracture behaviors of FRCC [1, 6, 19, 20].

Recently, carbon fiber (CF) has been drawing wide attention in industries such as ships, automobiles, civil engineering, and construction as well as aerospace due to its lightweight and high mechanical properties [21, 22]. It was once already reported that carbon fiber is very effective in improving the flexural, tensile, and shear strengths when used as cement-reinforcing materials, owing to its high physical properties and chemical stabilities [23–26]. However, when carbon fiber is applied as a construction material, there are some problems to consider despite the excellent mechanical properties it will provide. The carbon fiber, when used cement-reinforcing materials, has an effect of improving the mechanical performance by being uniformly dispersed in cement matrix and inducing bond between fibers and matrix. In particular, a decrease in compressive, flexural, and shear strengths may rather result if carbon fiber is not fully adhered to the cement matrix [27–29]. Therefore, the interfacial bonding force between fibers and matrix is so important that lots of studies on CFRM composites have been conducted and advanced worldwide. To improve the

interfacial bonding force between fibers and matrix, sizing treatment of carbon fibers is performed in this regard.

Although FRCC has been reviewed in the previous domestic and foreign studies, research studies to manufacture the carbon fiber with improved bond performance and developments to improve the mechanical performance of CFRM composites are still more or less insufficient [30, 31]. In Korea, the research data which specifically reviewed the bond properties between the carbon fiber and cement matrix are very limited [32]. In fact, there is a need to develop a method to improve the interfacial bonding force by coating the surface of carbon fiber with  $\text{SiO}_2$ , inducing by this reaction with limestone or  $\text{Ca}(\text{OH})_2$  in cement matrix and eventually increasing calcium silicate hydrate (C-S-H) gel.

Therefore, the main objective of this study is to develop CFRM composites that can improve the bond performance of carbon fiber and ultimately enhance the mechanical performance of mortar. This study provides a method for producing carbon fiber coated with  $\text{SiO}_2$  in order to improve the interfacial bonding force between fibers and matrix in cement matrix, and the mechanical properties of  $\text{SiO}_2$ -coated CFRM composites and uncoated CFRM composites with different fiber lengths (6 mm and 12 mm) and fiber volume fractions (0.5%, 1.0%, 1.5%, and 2.0%) are compared and analyzed in this study. Then, after the strength test, the fracture surface of the hardened CFRM composites was observed by an SEM.

## 2. Materials and Methods

In this study, it was found from checking the mechanical properties of  $\text{SiO}_2$ -coated CFRM composites and uncoated CFRM composites that the lengths of fibers were 6 mm and 12 mm, and the fiber volume fractions varied from 0.5 to 2.0% by 0.5%. This was compared and reviewed with plain mortar. The flow, air content, and unit weight were measured in the fresh mortar state, while the compressive and flexural strengths were measured in the hardened mortar state. Besides, the surface of the carbon fiber was observed by SEM imaging.

### 2.1. Materials

**2.1.1. Cement.** The cement used in this study is Ordinary Portland Cement (OPC) produced by S Co., Ltd., with a specific gravity of 3.13 and a powder density of  $3,860 \text{ cm}^2/\text{g}$ . The chemical composites of cement are shown in Table 1.

**2.1.2. Fine Aggregate.** The standard sand produced by Jumunjin was used as fine aggregate to make uniform mortar. The specific gravity of fine aggregate in the dry saturated state of the surface was 2.65, and the physical properties of fine aggregate are shown in Table 2.

**2.1.3. Carbon Fiber.** The high-strength carbon fiber based on polyacrylonitrile (PAN) used in this study was manufactured by T company in Japan, which has a tensile strength of

TABLE 1: Chemical composites of cement (%).

| SiO <sub>2</sub> | Al <sub>2</sub> O <sub>3</sub> | Fe <sub>2</sub> O <sub>3</sub> | CaO   | MgO  | Na <sub>2</sub> O | K <sub>2</sub> O | SO <sub>3</sub> | F-CaO | Ignition loss |
|------------------|--------------------------------|--------------------------------|-------|------|-------------------|------------------|-----------------|-------|---------------|
| 21.47            | 6.21                           | 3.70                           | 59.24 | 2.08 | 0.13              | 1.08             | 2.48            | 0.57  | 2.87          |

TABLE 2: Physical properties of fine aggregate.

| Size (mm) | Unit mass (kg/m <sup>3</sup> ) | Density (g/cm <sup>3</sup> ) | Fineness modulus (FM) |
|-----------|--------------------------------|------------------------------|-----------------------|
| 2 $\leq$  | 1,490                          | 2.65                         | 2.78                  |

4,900 MPa and an elastic modulus of 230 GPa. To secure a uniform carbon fiber length, fibers were cut into the average lengths of 6 mm and 12 mm prior to use. In order to secure the length of the carbon fiber uniformly, it was cut from the long fibers to 6 mm and 12 mm in average length. The physical properties of carbon fiber are shown in Table 3.

**2.1.4. Surface Modification of Carbon Fiber.** In order to coat the surface of carbon fiber with a sizing agent, the reagents and materials used in this study are colloidal SiO<sub>2</sub> sol (ss-sol 30a, 30%, S-Chemtech Co., Ltd.) in which nano-SiO<sub>2</sub> particles having a size of 10 nm are dispersed, and nitric acid (HNO<sub>3</sub>, 60%, Samchun Chemical) was used as a catalyst. GPTMS (99.9%, Sigma-Aldrich) was employed as a silane coupling agent, EDA (99.9%, Sigma-Aldrich) as a hardener, and ethanol (EtOH, 99.0%, Samchun Chemical) as a solvent, respectively. The reagent was used as such without purification and chemical treatment. SiO<sub>2</sub> sol was effective for consistently synthesizing high-purity SiO<sub>2</sub> particles at low temperatures. Based on the reinforcing mechanism of the modified carbon fiber, the SiO<sub>2</sub> particles produced on the surface of carbon fiber react with the hydration product Ca(OH)<sub>2</sub> in cement matrix, forming by thus a C-S-H gel which could improve the interfacial bonding force between fibers and matrix. After removing first all impurities attached to carbon fiber using acetone, the carbon fiber was oxidized by immersing it in a nitric acid solution for 24 hours to increase the surface activity, and the oxidized carbon fiber was washed with distilled water and dried in an oven at the temperature of 110°C. Then, the dried carbon fiber was dipped in the hydrophilic SiO<sub>2</sub>-coating solution synthesized through the above process for 3 hours to adhere the SiO<sub>2</sub> particles to the surface of the carbon fiber in order to surface-modify the carbon fiber with hydrophilicity. Subsequent to being hardened in an oven at 80°C for 1 hour, the carbon fiber was washed again with distilled water and dried at 120°C for 2 hours in the final process. Figure 2 shows the SiO<sub>2</sub>-coated carbon fiber and uncoated carbon fiber used in this experiment.

## 2.2. Methods

**2.2.1. Mix Proportions and Preparation of Specimens.** The mix proportions of mortar applied in this experiment are shown in Table 4. The water-cement ratio (W/C) was kept constant (equal to 0.5) for all mixtures according to the test regulations of KS L ISO 679 [33], and the ratio (mass ratio) of cement:standard sand:water = 1 : 3 : 0.5 was fixed. At this

TABLE 3: Physical properties and shapes of carbon fiber.

| Diameter ( $\mu$ m) | Density (kg/m <sup>3</sup> ) | Tensile strength (MPa) | Elastic modulus (GPa) | Elongation (%) |
|---------------------|------------------------------|------------------------|-----------------------|----------------|
| 7 $\pm$ 2           | 1,800                        | 4,900                  | 230                   | 2.1            |



FIGURE 2: Shapes of carbon fibers used in this experiment: (a) SiO<sub>2</sub>-coated carbon fibers (6 mm and 12 mm) and (b) uncoated carbon fibers (6 mm and 12 mm).

time, coarse aggregate was not used. That is, the amount of each batch material in the mixing ratio corresponds to 450  $\pm$  2 g of cement, 1,350  $\pm$  5 g of sand, and 225  $\pm$  1 g of water. The target flow value was mixed to be more than 190 mm or more. The amount of admixture added was adjusted to 1.0% of the cement mass, and in case of plain mortar, no particular admixture was added. The admixture used to ease the fluidity of carbon fiber is light yellow liquid, high-performance AE water reducing agent having a specific gravity of 1.04 and pH 5.0  $\pm$  1.5 in a series of polycarboxylic acid manufactured by D Co., Ltd., in Korea. Figure 3 shows the main experimental process and casting progress of each step for manufacturing of CFRM composite specimens. As for the mixing method, cement and fine aggregate were added first and then mixed, dried for 90 seconds. In order to secure dispersibility of fibers, carbon fibers were added and mixed for 60 seconds. Then, the blended water and admixture were added and immediately mixed for 90 seconds. Following the 30-second pause, the attached mortar was removed and finally a mixer was operated again for further 60 seconds. The total mixing time was about 5 minutes. The specimens were demolded after 24 hours and immersed in a water tank with the temperature maintained at 20  $\pm$  2°C constantly to perform underwater curing for 28 days of age.

**2.2.2. Test of Flow and Unit Weight.** In order to evaluate the fluidity performance of mortar, a flow test was conducted according to the test method of the “testing method for

TABLE 4: Mix proportions of mortar.

| Type of mortar | W/C (%) | C : S ratio | Fiber volume fractions (% , in vol) | Fiber lengths (mm) | Content of SP (cement $\times$ 1.0%) |
|----------------|---------|-------------|-------------------------------------|--------------------|--------------------------------------|
| CC             | 50      | 1 : 3       | 0.5                                 | 6, 12              | 1.0                                  |
|                |         |             | 1.0                                 |                    |                                      |
|                |         |             | 1.5                                 |                    |                                      |
|                |         |             | 2.0                                 |                    |                                      |
|                |         |             | 0.5                                 |                    |                                      |
| UC             |         |             | 1.0                                 |                    |                                      |
|                |         |             | 1.5                                 |                    |                                      |
|                |         |             | 2.0                                 |                    |                                      |
| $p$            |         |             | —                                   |                    | —                                    |

CC is the SiO<sub>2</sub>-coated carbon fiber mortar, UC is the uncoated carbon fiber mortar,  $p$  is the plain mortar, C : S is the cement to fine aggregate ratio, and SP is the superplasticizer

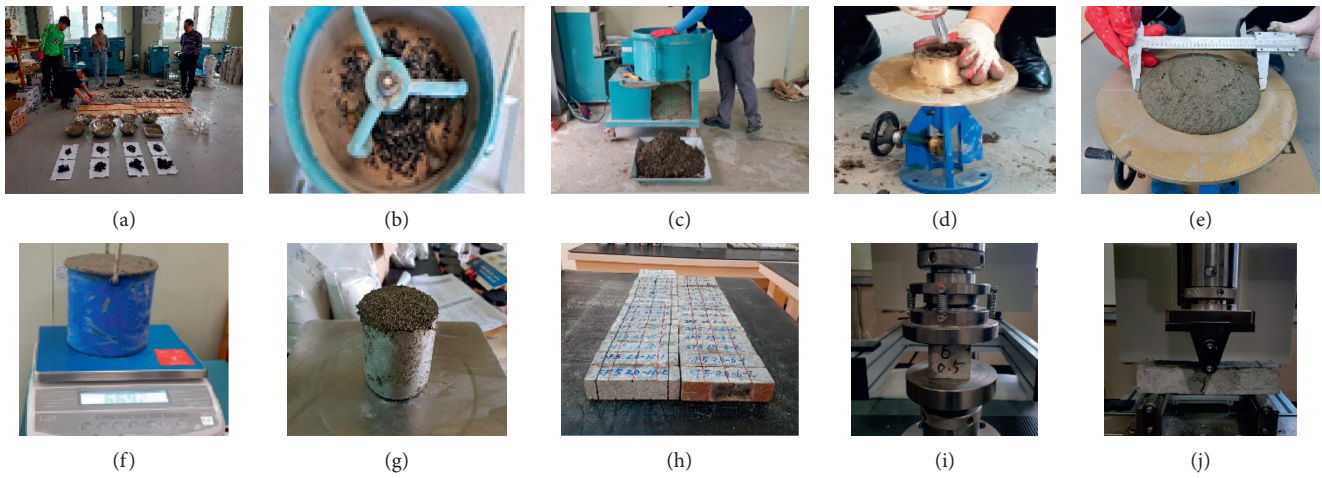


FIGURE 3: Main experimental process and casting progress of each step for manufacturing of CFRM composite specimens: (a) material metering, (b) fiber mixing, (c) finish mixing, (d) compaction, (e) flow test, (f) unit weight test, (g) air content test, (h) finish of specimens, (i) compressive test, and (j) flexural test.

compressive hydraulic cement mortar” in KS L 5105-2007 using the flow table specified in the “flow table for use in tests of hydraulic cement” in KS L 5111-2017, and a unit weight test was also performed according to the “standard test method for unit weight and air content of fresh concrete” in KS F 2409-2016.

**2.2.3. Test of Air Content.** Air content was measured using a cylindrical vessel capable of securing  $400 \pm 1$  mL of water at 23°C, having a diameter of  $76 \pm 1.5$  mm and a depth of 88 mm according to the test method specified in the “testing method for air content of hydraulic cement mortar” in KS L 3136-2005:

$$\text{air content (\%)} = 100 - \omega \left( \frac{182.7 + p}{2000 + 4p} \right), \quad (1)$$

where  $\omega$  is the mass ( $g$ ) of 400 mL mortar and  $p$  is the percentage of mixed water on the basis of cement.

**2.2.4. Test of CFRM Composite Mechanical Properties.** The compressive and flexural strength test of mortar was performed by preparing a mold according to the test method of KS L ISO 679 [33], and the strengths were all measured at

28 days of age. The cured cubic specimens of  $40 \times 40 \times 160$  mm were tested using a universal tester with a capacity of 100 kN (MTDI Co., Ltd., Korea, UT-100F). The flexural strength test was carried out on the basis of a three-point loading, and the specimen of 120 mm in length and 40 mm in height was loaded at a speed of 50 N/s. After the flexural strength test, a compressive strength test was conducted with a cut specimen. In the compressive strength test, the load area was  $1,600 \text{ mm}^2$ , and the speed was 2,400 N/s.

**2.2.5. SEM Observation.** SEM images were photographed to confirm whether the SiO<sub>2</sub> particles were coated on the surface of carbon fiber. The equipment used for analysis was MIRA LMH high-resolution SEM model of TESCAN. Besides, after the fibers obtained by pulverization of CFRM composite specimens were dried and coated with platinum in a vacuum state, it was observed whether the SiO<sub>2</sub> particles remained still attached to the surface of carbon fiber.

### 3. Results and Discussion

**3.1. Surface Topography of SiO<sub>2</sub>-Coated Carbon Fiber.** Figure 4 shows a photograph of the surface topography for SiO<sub>2</sub>-coated carbon fiber measured by the SEM. Figure 4(a)

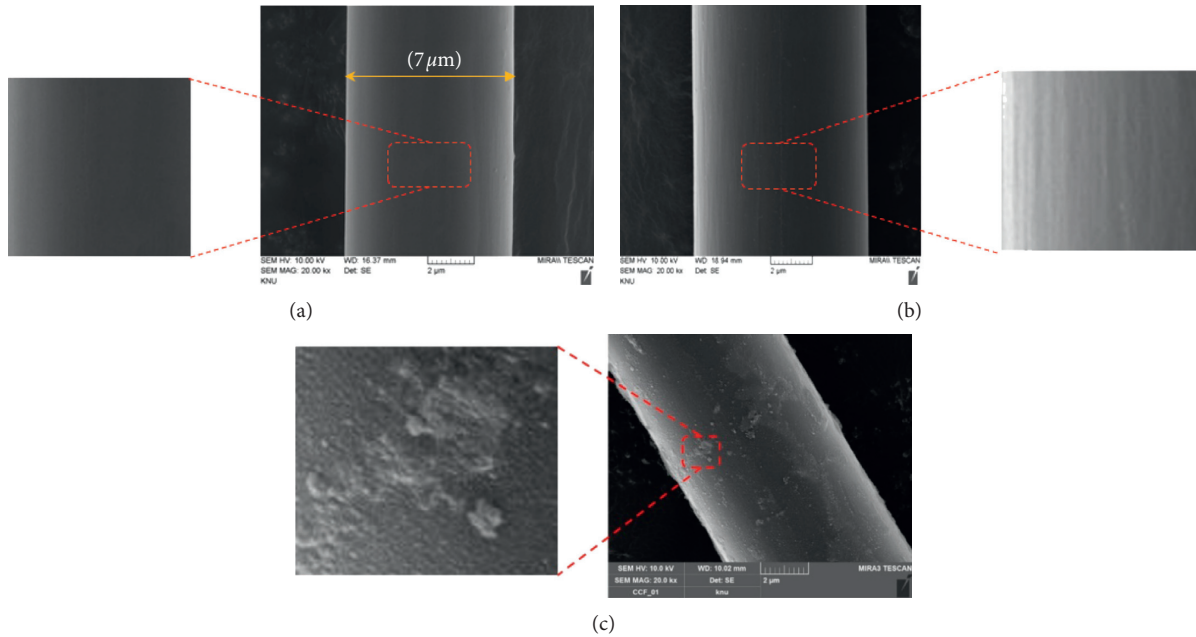


FIGURE 4: Surface topography of carbon fibers (20000 times): (a) uncoated carbon fiber, (b) nitric acid-treated carbon fiber, and (c) SiO<sub>2</sub>-coated carbon fiber.

shows an uncoated carbon fiber, Figure 4(b) shows a carbon fiber pretreated with nitric acid, and Figure 4(c) shows a carbon fiber coated with SiO<sub>2</sub>, observed by the SEM, respectively. The uncoated carbon fiber surface was neat and smooth, with a diameter of approximately 7 μm as shown in Figure 4(a). Compared to uncoated carbon fiber of Figure 4(a), the carbon fiber pretreated with nitric acid in Figure 4(b) has a string in the axial direction, increasing the surface roughness of carbon fiber. The objective of the pretreatment with nitric acid as shown in Figure 4(b) is to intensify roughness and to increase the number of COOH or -OH functional groups on the surface of carbon fibers by means of oxidation reaction in order to make SiO<sub>2</sub> particles easily attached to it. As shown in Figure 4(c), it can be seen that, in case of SiO<sub>2</sub>-coated carbon fiber, particles of several tens of nanometers in size are spread entirely and attached to the surface of carbon fibers.

### 3.2. Properties of Fresh Mortar

**3.2.1. Fluidity of Mortar.** Figure 5 shows the test results of flow values of SiO<sub>2</sub>-coated carbon fiber mortar and uncoated carbon fiber mortar with different fiber lengths and fiber volume fractions compared to plain mortar. The flow values were calculated from the average values measured in four directions, and the flow value for mixture of plain mortar was 192 mm, which satisfies more than the target flow value of 190 mm. On the other hand, the flow value for mixture of SiO<sub>2</sub>-coated carbon fiber mortar was 114 to 160 mm, while that of uncoated carbon fiber mortar was measured to be 103~146 mm. As shown in Figure 5, the variation in flow value at the lengths of fibers (6 mm, 12 mm) was insignificant but tended to decrease significantly as the fiber volume

fractions increased. When carbon fibers were mixed in the ratio of 2.0% particularly, their flow was drastically reduced and fluidity was very disadvantageous as far as fluidity of fire balls and nonhydrophilicity of the fibers are concerned. These results are due to the fiber balls caused by increase in the viscosity of mortar and by partial absorption of the mixed water during the mixing process, which is considered to show a lower flow value than the plain mortar. Figure 6 shows pictures that compare flows of SiO<sub>2</sub>-coated carbon fiber mortar, uncoated carbon fiber mortar, and plain mortar, respectively. The uncoated carbon fiber mortar was not sufficiently mixed, and some fibers were exposed to the surface. When the reinforced fibers are uniformly dispersed as the flow value increases, it may be evaluated that the flow value of a mortar increases accordingly. As a consequence, the optimum dispersibility and workability could be obtained. In dry mixing, fiber balls and maldistribution of fibers would occur, and even in wet mixing, there was a tendency to make smooth dispersibility difficult; entanglement between each fiber could easily occur due to the increased amount of mixed fibers, by thus affecting workability adversely.

**3.2.2. Unit Weight of Mortar.** Figure 7 shows the test results of unit weight of SiO<sub>2</sub>-coated carbon fiber mortar and uncoated carbon fiber mortar with different fiber lengths and fiber volume fractions compared to plain mortar. As shown in Figure 7, regardless of whether the fibers were coated, variation in the unit weight was slight in fiber lengths of 6 mm and 12 mm but tended to decrease significantly as the fiber volume fractions increased. Compared to plain mortar, the unit weight was significantly reduced. This is due to the difference in the density of cement and carbon fiber, and it is thought that the unit weight is reduced due to the

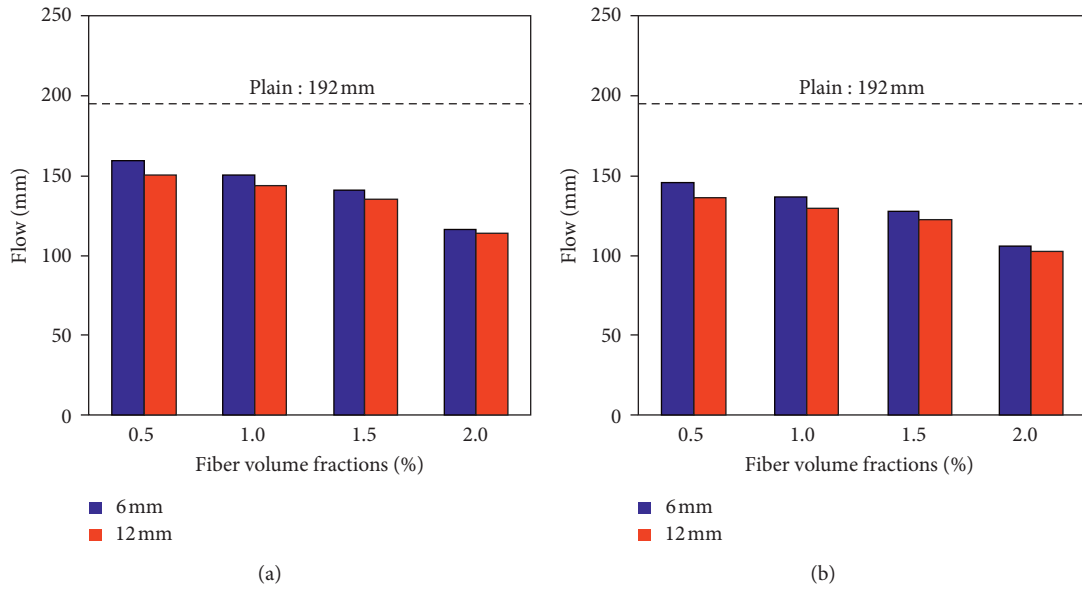


FIGURE 5: Flow test results with different fiber lengths and fiber volume fractions: (a) SiO<sub>2</sub>-coated carbon fiber and (b) uncoated carbon fiber.

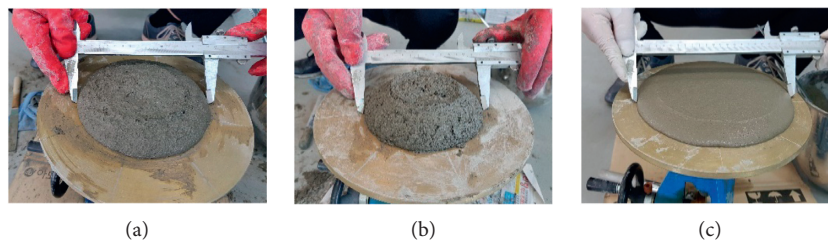


FIGURE 6: Flow test of mortar samples: (a) SiO<sub>2</sub>-coated carbon fiber mortar, (b) uncoated carbon fiber mortar, and (c) plain mortar.

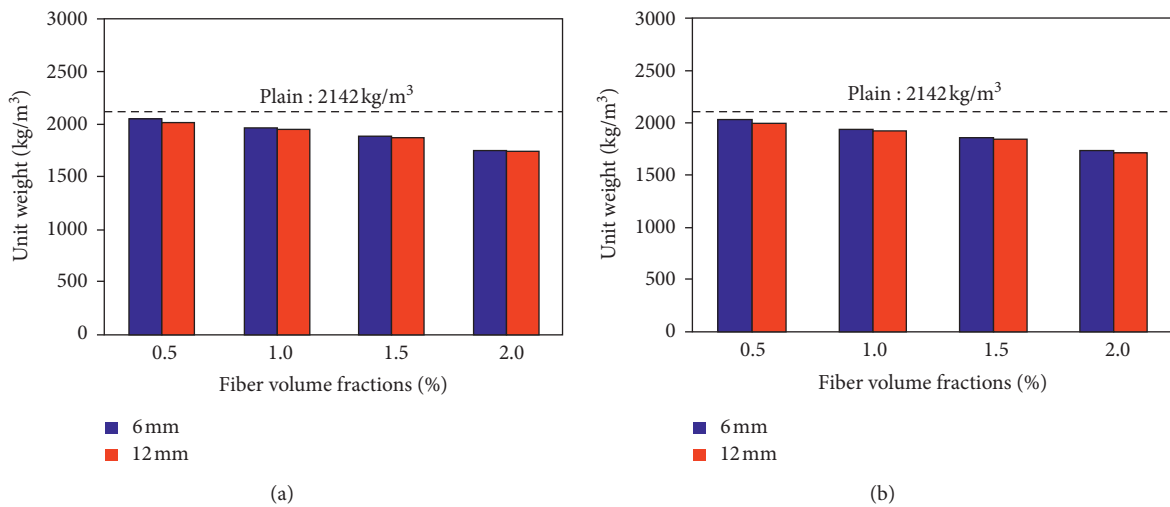


FIGURE 7: Unit weight test results with different fiber lengths and fiber volume fractions: (a) SiO<sub>2</sub>-coated carbon fiber and (b) uncoated carbon fiber.

large amount of incorporated carbon fibers with a relatively smaller density than cement. Regardless of whether the fibers were coated or not, the unit weight of carbon fiber mortar could be reduced by about 4 ~ 5% as fiber volume fractions increased and by about 18 ~ 20% of plain mortar.

3.2.3. *Air Content of Mortar.* Figure 8 shows the test results of air content of SiO<sub>2</sub>-coated carbon fiber mortar and uncoated carbon fiber mortar with different fiber lengths and fiber volume fractions compared to plain mortar. As shown in Figure 8, regardless of whether the fibers were coated or not,

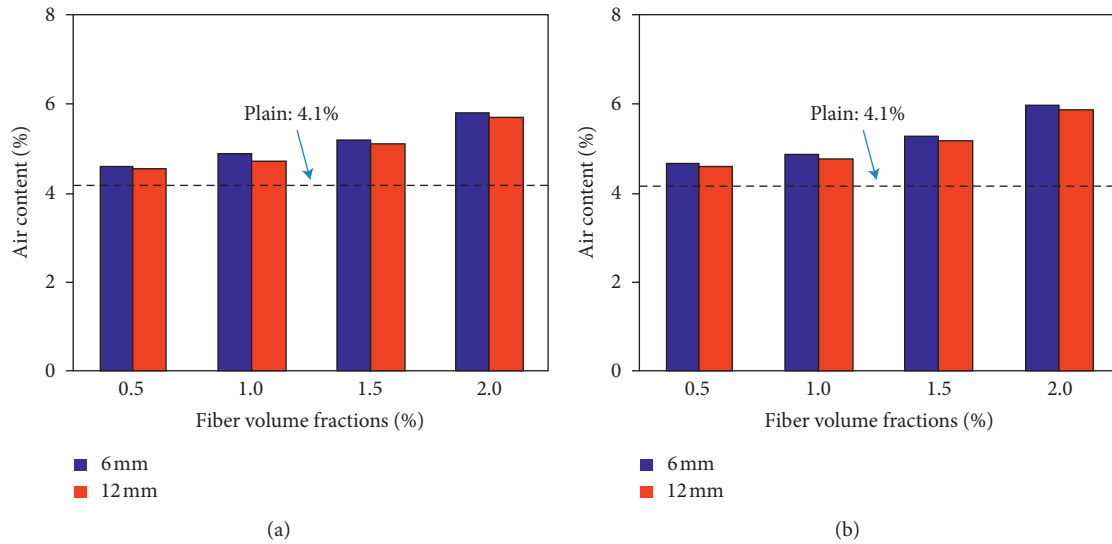


FIGURE 8: Air content test results with fiber lengths and fiber volume fractions: (a) SiO<sub>2</sub>-coated carbon fiber and (b) uncoated carbon fiber.

variation in the air content was slight when the lengths of fibers were 6 mm and 12 mm but tended to increase a little as the fiber volume fractions increased. Compared to plain mortar, air content increased for both. The test results estimated that the effect on the air content in the case of carbon fiber mortar was not so much, and the air content did not vary significantly in line with the increasing rate of fiber mixture.

### 3.3. Properties of Hardened Mortar

**3.3.1. Properties of the Compressive Strength.** Figure 9 shows the test results of the compressive strength of SiO<sub>2</sub>-coated CFRM composite specimens and uncoated CFRM composite specimens with different fiber lengths and fiber volume fractions compared to plain mortar specimens. The compressive strength of plain mortar specimens at 28 days of age was measured to be 30.6 MPa in average. As shown in Figure 9(a), the compressive strength was reduced compared to plain mortar specimens, except for the CFRM composite specimens with 0.5% of fibers and SiO<sub>2</sub>-coated carbon fiber. Whether or not fibers were coated, the compressive strength of the CFRM composite specimens showed an overall decrease in strength as the fiber volume fractions increased. This is thought to be caused by the carbon fiber, and the strength of which is lowered because the interfacial bonding force between fibers and matrix in the mortar was weakened after hardening due to the nonhydrophilic material on the surface of carbon fibers. These results were also reported in the previous studies [34, 35], which revealed that the dispersibility of fibers decreased and more agglomeration was caused since the fiber volume fractions become higher from a certain amount, which resulted in decrease of the compressive strength. As the flow value decreased due to fiber volume fractions, the quality of material that could affect the compressive strength was uneven and, as a consequence, the compressive strength decreased accordingly. Regardless of whether the fibers were coated or not, the compressive

strength tended to decrease rapidly due to high fiber volume fractions when fibers were mixed in the ratio of 1.5% and 2.0%. In the event fibers were mixed with 2.0%, particularly, it was difficult to uniformly disperse the fibers in cement matrix. Moreover, fiber balls occurred and the compressive strength was rapidly reduced due to insufficient dispersion. When the lengths of fibers are 6 mm and 12 mm, and they are mixed at 0.5% and 1.0%, the compressive strength was almost the same or slightly different, but when mixed at 2.0%, the compressive strength of fibers was reduced drastically by approximately 29.7 ~ 55.3% more than plain mortar specimens. Meanwhile, the use of 12 mm fibers was seen to be more efficient than that of 6 mm ones. Therefore, in case of the CFRM composite specimens, 0.5% and 1.0% are considered to be the most appropriate fiber volume fractions in terms of securing the compressive strength while maintaining the maximum workability. Concerning the tendency for the compressive strength to decrease rapidly due to high fiber volume fractions, it is required to conduct further studies to improve the strength.

**3.3.2. Properties of the Flexural Strength.** Figure 10 shows the test results of the flexural strength of SiO<sub>2</sub>-coated CFRM composite specimens and uncoated CFRM composite specimens with different fiber lengths and fiber volume fractions compared to plain mortar specimens. The flexural strength of plain mortar specimens at 28 days of age was measured to be 3.1 MPa in average. As shown in Figure 10, the flexural strength of SiO<sub>2</sub>-coated CFRM composite specimens demonstrated fairly higher value compared to the plain mortar specimen in all types except for uncoated CFRM composite specimens mixed with fibers of 6 mm length and in the ratio of 0.5%. In particular, the SiO<sub>2</sub>-coated CFRM composite specimens with fiber length of 12 mm and mixture of 1.5% had the highest flexural strength of about 4.9 MPa. It was analyzed that the flexural strength increased by 10.4% and 58.1%, respectively, compared to uncoated

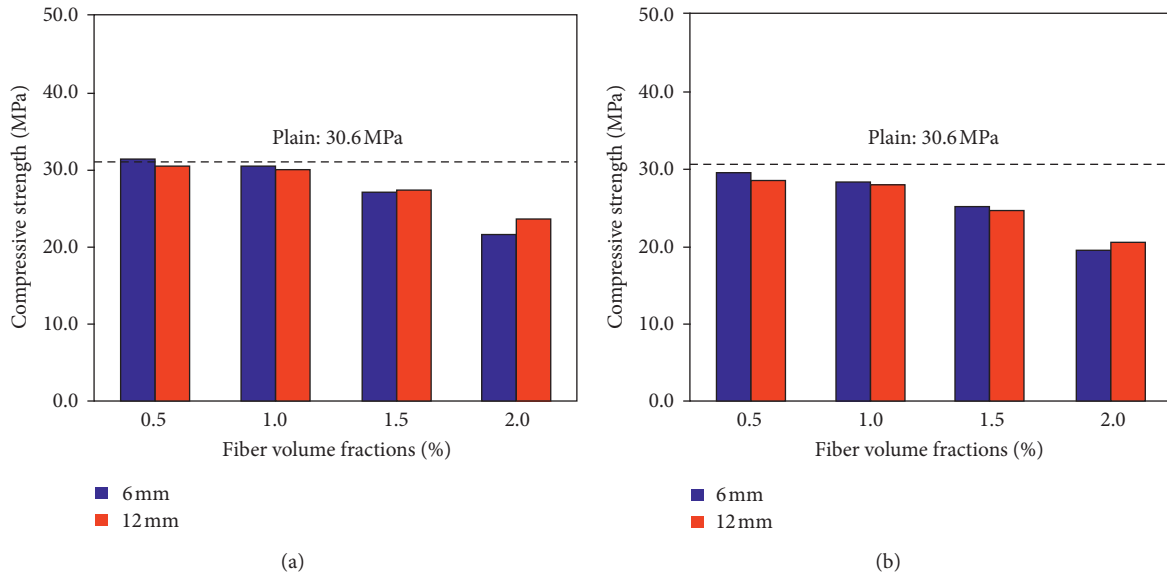


FIGURE 9: Relationships between compressive strengths of the CFRM composite specimens with different fiber lengths and fiber volume fractions: (a) SiO<sub>2</sub>-coated carbon fiber and (b) uncoated carbon fiber.

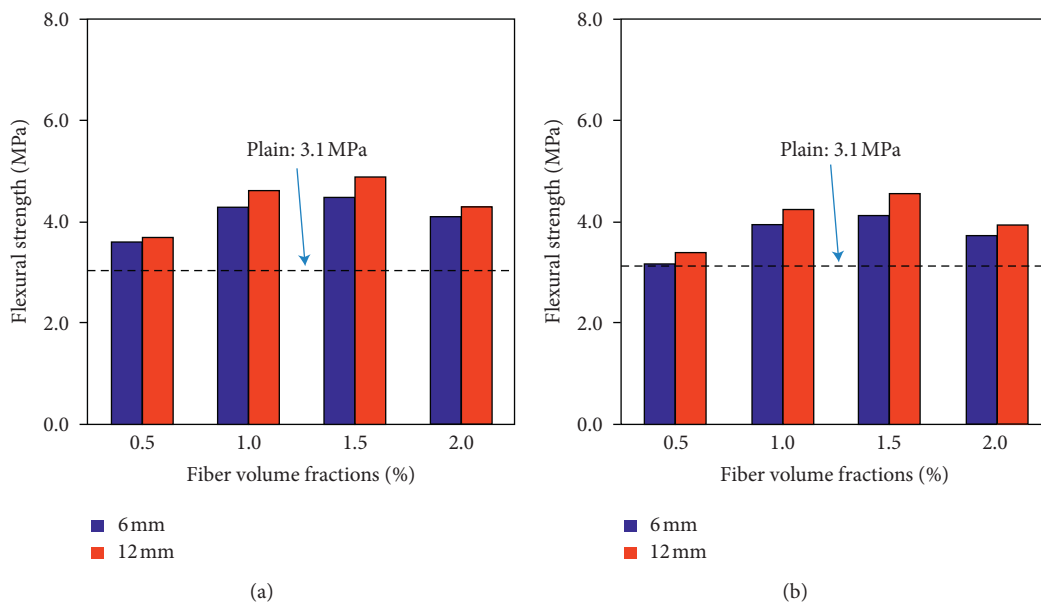


FIGURE 10: Relationships between flexural strengths of CFRM composite specimens with different fiber lengths and fiber volume fractions: (a) SiO<sub>2</sub>-coated carbon fiber and (b) uncoated carbon fiber.

CFRM composite specimens and plain mortar specimens. These results are judged to be because added fibers have a bridging effect to prevent the growth of cracks and improve the flexural strength through redistribution of stress. The flexural strength improved until the fiber volume fractions reached up to 1.5%, but the increasing effect would not be so great if the fiber volume fractions were greater than that. Actually, however, it was laid bare that the fibers with a length of 6 mm and mixing ratio of 2.0% had the least flexural strength because dispersibility and finishing performance were not favorable due to the high fiber volume fractions. Moreover, when the length of the fiber was 6 mm,

it could be confirmed that the flexural strength was lower than that of 12 mm. This is thought to be due to the bridging action between the fibers that could not be obtained sufficiently because the length of the fibers was reduced by 50% compared to the 12 mm fibers.

3.3.3. Relationship between the Compressive and Flexural Strengths. Table 5 summarizes the test data results of the compressive and flexural strengths of SiO<sub>2</sub>-coated CFRM composite specimens, uncoated CFRM composite specimens, and plain mortar specimens. For SiO<sub>2</sub>-coated CFRM

TABLE 5: Results of strength tests with different fiber lengths and fiber volume fractions.

| Type of mortar                                  | Fiber volume fractions<br>(%, in vol) | Fiber lengths<br>(mm) | Mortar strength<br>(MPa) |       | $f_c/f_r$ |
|---|---------------------------------------|-----------------------|--------------------------|-------|-----------|
|   |                                       |                       | $f_c$                    | $f_r$ |           |
| SiO <sub>2</sub> -coated carbon<br>fiber (CFRM) | 0.5                                   | 6                     | 31.4                     | 3.6   | 8.7       |
|   |                                       | 12                    | 30.4                     | 3.7   | 8.2       |
|   | 1.0                                   | 6                     | 30.5                     | 4.3   | 7.1       |
|   |                                       | 12                    | 30.0                     | 4.6   | 6.5       |
|   | 1.5                                   | 6                     | 27.1                     | 4.5   | 6.0       |
|   |                                       | 12                    | 27.3                     | 4.9   | 5.6       |
|   | 2.0                                   | 6                     | 21.6                     | 4.1   | 5.3       |
|   |                                       | 12                    | 23.6                     | 4.3   | 5.5       |
| Uncoated carbon<br>fiber (CFRM)                 | 0.5                                   | 6                     | 29.6                     | 3.2   | 9.3       |
|   |                                       | 12                    | 28.6                     | 3.4   | 8.4       |
|   | 1.0                                   | 6                     | 28.5                     | 3.9   | 7.3       |
|   |                                       | 12                    | 28.0                     | 4.2   | 6.7       |
|   | 1.5                                   | 6                     | 25.3                     | 4.1   | 6.2       |
|   |                                       | 12                    | 24.8                     | 4.5   | 5.5       |
|   | 2.0                                   | 6                     | 19.7                     | 3.7   | 5.3       |
|   |                                       | 12                    | 20.7                     | 3.9   | 5.2       |
| Plain mortar                                    | —                                     | —                     | 30.6                     | 3.1   | 9.9       |

$f_c$  is the average of the compressive strength measured at 28 days, and  $f_r$  is the average of the flexural strength measured at 28 days.

composite specimens at 28 days of age, the ratio of the flexural strength to the compressive strength was within the range of 1/5.3 ~ 1/8.7. On the other hand, the ratio of uncoated CFRM composite specimens was shown to be in the range of 1/5.2 to 1/9.3, indicating that the flexural strength increased a little compared to the 1/9.9 level of the plain mortar specimen. These results are assumed to be because the mixed fibers prevented crack propagation due to the bridging role and the flexural strength was improved through redistribution of stress. Regardless of whether the fibers were coated or not, the flexural strength was improved when fibers were mixed up at 1.5%, but the increasing effect was not so great when more fibers were mixed. In case of uncoated CFRM composite specimens having a fiber length of 6 mm and a mixture of 2.0%, it can be seen that the flexural strength was the lowest because of poor dispersion and finishing performance caused by high mixing ratio.

### 3.3.4. Flexural Stress-Displacement Relationship Curves.

Figure 11 shows the flexural stress-displacement relationship curves of a representative specimen based on a three-point loading test. In case of plain mortar specimens, the flexural stress increased linearly, and there was little displacement after reaching the maximum stress due to rapid brittle fracture at the same time as the flexural crack occurred. On the other hand, the CFRM composite specimens showed a behavior in which the stress decreased after arriving at the maximum stress, displacement increased to a certain extent, and then the descending slope fell down gradually, while displacement increased. In case of uncoated CFRM composite specimens, it can be seen that the displacement is subject to stress up to 1.7 mm, and the displacement of SiO<sub>2</sub>-coated CFRM composite specimens was found to resist up to 2.0 mm due to ductile properties. Therefore, the amount of displacement increased in the flexural stress and the

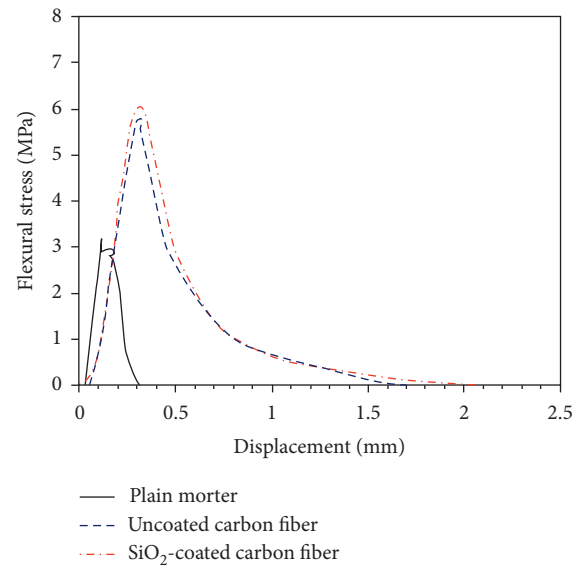


FIGURE 11: Flexural stress-displacement relationship curves.

displacement curve was found to be the largest for SiO<sub>2</sub>-coated CFRM composite specimens in the order of SiO<sub>2</sub>-coated CFRM composite specimens > uncoated CFRM composite specimens > plain mortar specimens.

3.4. SEM Observation. Figure 12 shows the microstructure of the fiber surface observed by using SEM after the strength test of SiO<sub>2</sub>-coated CFRM composite specimens and uncoated CFRM composite specimens. In general, the bond performance of reinforced fibers is affected by the interfacial bonding force between fibers and cement matrix. Therefore, to improve the interface bonding force between the fibers and matrix in the cement composites, sizing treatment of

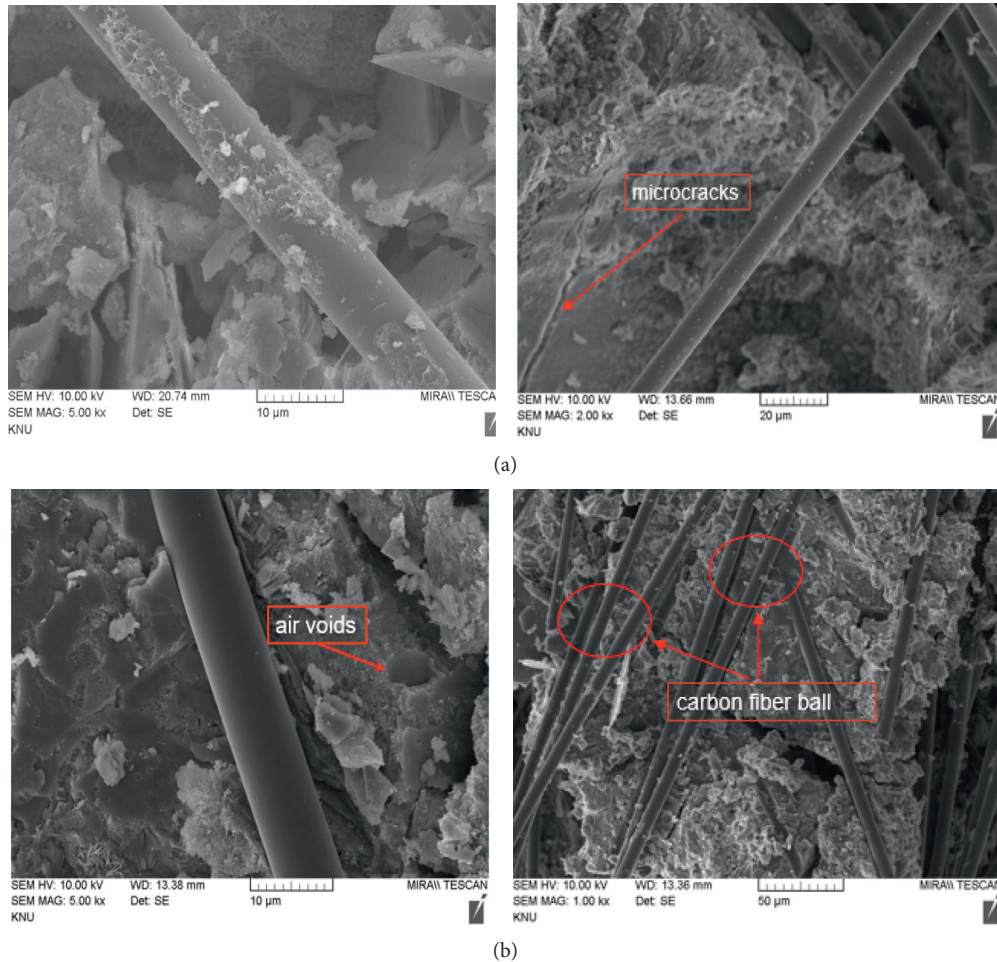


FIGURE 12: SEM images of CFRM composite specimens after strength tests (5000 or 1000 times): (a) SiO<sub>2</sub>-coated carbon fiber and (b) uncoated carbon fiber.

carbon fibers is performed. If the interfacial bonding force is large, the bond performance is excellent, whereas the bond performance is poor, if the interfacial bonding force is small. It is reported that the thickness between fibers and cement matrix interface is about 10 to 50 μm, and this interface thickness is known to affect strength and durability [36, 37]. As revealed in Figure 12(a), it can be seen that, in case of the SiO<sub>2</sub>-coated CFRM composite specimens, large and small C-S-H gels are uniformly distributed in a rough shape on the surface of fibers, and almost no pores can be observed. However, microcracks are shown to be occasionally occurring, though. It is thus made clear that the interfacial bonding force between fibers and matrix was improved owing to formation and increase of the cement hydration product. On the other hand, it was observed from Figure 12(b) that the fiber surface of uncoated CFRM composite specimens looked very clean and quite smooth and that a number of pores were formed. This is because the cement hydration product is difficult to crystallize and has a low affinity, so the interfacial bonding force between fibers and cement matrix is low. It appears therefore that fiber balls have occurred. As such, the SiO<sub>2</sub>-coated CFRM composite specimens showed better interfacial bonding force than the

uncoated CFRM composite specimens owing to the improved interfacial bonding force between fibers and cement matrix.

#### 4. Conclusions

In the present study, carbon fibers coated with SiO<sub>2</sub> as cement-reinforcing materials were manufactured, and the mechanical properties of SiO<sub>2</sub>-coated CFRM composites and uncoated CFRM composites with different fiber lengths and fiber volume fractions were compared and analyzed. The outcomes of the study may be summarized as follows:

- (1) The target flow value of plain mortar was satisfactory, but the flow values of SiO<sub>2</sub>-coated carbon fiber mortar and uncoated carbon fiber mortar decreased significantly as fiber volume fractions increased. In this regard, there is a need for a means to insure fluidity with increasing carbon fiber volume fractions. In addition, compared to plain mortar, the unit weight decreased by about 1820% as the fiber volume fractions increased, while the air content increased a little bit.

- (2) Regardless of whether the fibers were coated, the compressive strength of CFRM composite specimens decreased somewhat compared to plain mortar specimens, and there was a strong tendency that the more the fiber volume fractions increased, the more the compressive strength decreased. In particular, when the fiber length was 6 mm and mixed at 2.0%, the compressive strength was significantly reduced.
- (3) The flexural strength of SiO<sub>2</sub>-coated CFRM composite specimens was higher than that of uncoated CFRM composite specimens and plain mortar specimens by 10.4% and 58.1%, respectively. Particularly, when the fiber length was 12 mm and mixed at 1.5 %, the highest flexural strength could be obtained.
- (4) The ratio of the flexural strength to the compressive strength is approximately 1/5.3 ~ 1/8.7 and 1/5.2 ~ 1/9.3 for SiO<sub>2</sub>-coated CFRM composite specimens and uncoated CFRM composite specimens, respectively, confirming that the flexural strength increased significantly compared to the 1/9.9 level of plain mortar specimens.
- (5) The SEM observation result showed that, in case of SiO<sub>2</sub>-coated CFRM composite specimens, a number of crystals of the cement hydration product were formed on the surface of the carbon fiber, which pushed the interfacial bonding force higher than that of the uncoated CFRM composite specimens.

## Data Availability

The data used to support the findings of this study are available from the corresponding author upon request.

## Conflicts of Interest

The authors declare that there are no conflicts of interest regarding the publication of this paper.

## Acknowledgments

This research was supported by the Basic Science Research Program through the National Research Foundation of Korea (NRF) funded by the Ministry of Education (grant no. NRF-2018R1A6A1A03025542).

## References

- [1] A. Abrishambaf, M. Pimentel, and S. Nunes, "Influence of fibre orientation on the tensile behaviour of ultra-high performance fibre reinforced cementitious composites," *Cement and Concrete Research*, vol. 97, pp. 28–40, 2017.
- [2] D. j. Kim, A. E. Naaman, and S. EL-Tawil, "Comparative flexural behavior of four fiber reinforced cementitious composites," *Cement and Concrete Composites*, vol. 30, no. 10, pp. 917–928, 2008.
- [3] G. H. Heo, J. G. Park, and C. G. Kim, "Evaluating the resistance performance of the VAEPC and the PAFRC composites against a low-velocity impact in varying temperature," *Advances in Civil Engineering*, vol. 2020, Article ID 7901512, 15 pages, 2020.
- [4] L. Lavagna, S. Musso, G. Ferro, and M. Pavese, "Cement-based composites containing functionalized carbon fibers," *Cement and Concrete Composites*, vol. 88, pp. 165–171, 2018.
- [5] L. Sun, Q. Hao, J. Zhao, D. Wu, and F. Yang, "Stress strain behavior of hybrid steel-PVA fiber reinforced cementitious composites under uniaxial compression," *Construction and Building Materials*, vol. 188, pp. 349–360, 2018.
- [6] S.-T. Kang, Y. Lee, Y.-D. Park, and J.-K. Kim, "Tensile fracture properties of an ultra high performance fiber reinforced concrete (UHPFRC) with steel fiber," *Composite Structures*, vol. 92, no. 1, pp. 61–71, 2010.
- [7] A. M. Brandt, "Fibre reinforced cement-based (FRC) composites after over 40 years of development in building and civil engineering," *Composite Structures*, vol. 86, no. 13, pp. 3–9, 2008.
- [8] H. Li, R. Mu, L. Qing, H. Chen, and Y. Ma, "The influence of fiber orientation on bleeding of steel fiber reinforced cementitious composites," *Cement and Concrete Composites*, vol. 92, pp. 125–134, 2018.
- [9] K. Hannawi, H. Bian, W. P. Agbodjan, and B. Raghavan, "Effect of different types of fibers on the microstructure and the mechanical behavior of Ultra-High Performance Fiber-Reinforced Concretes," *Composites Part B: Engineering*, vol. 86, pp. 214–220, 2016.
- [10] M. Cao, Y. Mao, M. Khan, W. Si, and S. Shen, "Different testing methods for assessing the synthetic fiber distribution in cement-based composites," *Construction and Building Materials*, vol. 184, pp. 128–142, 2018.
- [11] A. Bentur and S. Mindess, *Fibre Reinforced Cementitious Composites*, Elsevier Applied Science, London, UK, 1990.
- [12] A. Bhutta, M. Farooq, C. Zanotti, and N. Banthia, "Pull-out behavior of different fibers in geopolymers mortars: effects of alkaline solution concentration and curing," *Materials and Structures*, vol. 50, no. 1, pp. 1–13, 2017.
- [13] ACI Committee 544, *Fibre Reinforced Concrete*, Vol. SP-81, America Concrete Institute, Farmington Hills, MI, USA, 1984.
- [14] A. E. Naaman, "Toughness, ductility, surface energy and deflection-hardening FRC composites," in *Proceedings of the JCI International Workshop on Ductile Fiber-Reinforced Cementitious Composites (DFRCC), Application and Evaluation*, Japan Concrete Institute, Tokyo, Japan, pp. 33–57, October 2002.
- [15] D. L. Naik, A. Sharma, R. R. Chada, R. Kiran, and T. Sirotiak, "Modified pullout test for indirect characterization of natural fiber and cementitious matrix interface properties," *Construction and Building Materials*, vol. 208, pp. 381–393, 2019.
- [16] D.-Y. Yoo, J.-J. Park, S.-W. Kim, and Y.-S. Yoon, "Combined effect of expansive and shrinkage-reducing admixtures on the properties of ultra high performance fiber-reinforced concrete," *Journal of Composite Materials*, vol. 48, no. 16, pp. 1981–1991, 2014.
- [17] W. Zemei, K. K. Henri, and S. Caijun, "Effect of nano-SiO<sub>2</sub> particles and curing time on development of fiber-matrix bond properties and microstructure of ultra-high strength concrete," *Cement Concrete Research*, vol. 95, pp. 247–256, 2017.
- [18] Z. Rong, W. Sun, H. Xiao, and G. Jiang, "Effects of nano-SiO<sub>2</sub> particles on the mechanical and microstructural properties of ultra-high performance cementitious composites," *Cement and Concrete Composites*, vol. 56, pp. 25–31, 2015.
- [19] A. Bhutta, P. H. R. Borges, C. Zanotti, M. Farooq, and N. Banthia, "Flexural behavior of geopolymers composites

- reinforced with steel and polypropylene macro fibers,” *Cement and Concrete Composites*, vol. 80, pp. 31–40, 2017.
- [20] J. P. Won, B. T. Hong, T. J. Choi, S. J. Lee, and J. W. Kang, “Flexural behavior of amorphous micro-steel fibre-reinforced cement composites,” *Composites Structure*, vol. 94, pp. 1443–1449, Elsevier, Amsterdam, Netherlands, 2012.
- [21] B. Gao, R. Zhang, M. He et al., “Interfacial microstructure and mechanical properties of carbon fiber composites by fiber surface modification with poly (amidoamine)/polyhedral oligomeric silsesquioxane,” *Composites Part A: Applied Science and Manufacturing*, vol. 90, pp. 653–661, 2016.
- [22] H. Yao, X. Sui, Z. Zhao et al., “Optimization of interfacial microstructure and mechanical properties of carbon fiber/epoxy composites via carbon nanotube sizing,” *Applied Surface Science*, vol. 347, pp. 583–590, 2015.
- [23] G. A. Galhano, L. F. Valandro, R. M. de Melo, R. Scotti, and M. A. Bottino, “Evaluation of the flexural strength of carbon fiber-, quartz fiber-, and glass fiber-based posts,” *Journal of Endodontics*, vol. 31, no. 3, pp. 209–211, 2005.
- [24] J. Sun, F. Zhao, Y. Yao, X. Liu, Z. Jin, and Y. Huang, “A two-step method for high efficient and continuous carbon fiber treatment with enhanced fiber strength and interfacial adhesion,” *Materials Letters*, vol. 196, no. 1, pp. 46–49, 2017.
- [25] J. Sun, F. Zhao, Y. Yao, Z. Jin, X. Liu, and Y. Huang, “High efficient and continuous surface modification of carbon fibers with improved tensile strength and interfacial adhesion,” *Applied Surface Science*, vol. 412, no. 1, pp. 424–435, 2017.
- [26] X. Fu, W. Lu, and D. D. L. Chung, “Improving the tensile properties of carbon fiber reinforced cement by ozone treatment of the fiber,” *Cement and Concrete Research*, vol. 26, no. 10, pp. 1485–1488, 1996.
- [27] W. Chuang, J. G. Sheng, L. B. Liang et al., “Dispersion of carbon fibers and conductivity of carbon fiber-reinforced cement-based composites,” *Ceramics International*, vol. 43, no. 17, pp. 15122–15132, 2017.
- [28] R. Liu, H. G. Xiao, H. Li et al., “Effects of nano-SiO<sub>2</sub> on the permeability-related properties of cement-based composites with different water/cement ratios,” *Journal of Materials Science*, vol. 53, no. 13, pp. 4974–4986, 2018.
- [29] T. Sugama, L. E. Kukacka, N. Carciello, and D. Stathopoulos, “Interfacial reactions between oxidized carbon fibers and cements,” *Cement and Concrete Research*, vol. 19, no. 3, pp. 355–365, 1989.
- [30] M. Balapour, A. Joshaghani, and F. Althoey, “Nano-SiO<sub>2</sub> contribution to mechanical, durability, fresh and microstructural characteristics of concrete: a review,” *Construction and Building Materials*, vol. 181, pp. 27–41, 2018.
- [31] M. Lu, H. Xiao, M. Liu, X. Li, H. Li, and L. Sun, “Improved interfacial strength of SiO<sub>2</sub> coated carbon fiber in cement matrix,” *Cement and Concrete Composites*, vol. 91, pp. 21–28, 2018.
- [32] G.-H. Heo, K.-C. Song, J.-G. Park, J.-H. Park, and H.-M. Jun, “Effect of mechanical properties of SiO<sub>2</sub> coated carbon fiber reinforced mortar composites,” *Journal of the Korea Concrete Institute*, vol. 32, no. 1, pp. 65–76, 2020.
- [33] KS L ISO 679, *Methods of Testing Cements-Determination of Strength*, Korean Standards Association, Seoul, Republic of Korea, 2016.
- [34] M. Boulfiza, N. Banthia, and K. Sakai, “Application of continuum damage mechanics to carbon fiber-reinforced cement composites,” *ACI Materials Journal*, vol. 97, no. 3, pp. 245–253, 2000.
- [35] S. Y. Lee and Y. D. Park, “Mechanical properties of high strength carbon fiber reinforced cement composites,” *RIST Report*, vol. 8, no. 2, pp. 321–330, 1994.
- [36] K. L. Scrivener, A. K. Crumbie, and P. Laugesen, “The interfacial transition zone (ITZ) between cement paste and aggregate in concrete,” *Interface Science*, vol. 12, no. 4, pp. 411–421, 2004.
- [37] P. K. Metha, *Concrete-Structure, Properties, and Materials*, Prentice-Hall, Upper Saddle River, NJ, USA, 1986.